The International Journal of Advanced Manufacturing Technology (2018) 95:2757–2766
https://doi.org/10.1007/s00170-017-1431-6

ORIGINAL ARTICLE

The influence of bending mode ultrasonic-assisted friction stir welding of Al-6061-T6 alloy on residual stress, welding force and macrostructure

I. Alinaghian[1] · M. Honarpisheh[1] · S. Amini[1]

Received: 12 July 2017 / Accepted: 20 November 2017 / Published online: 27 November 2017

Abstract
Residual stress can affect the properties and performance of materials. Since it is an important factor in all welding processes, either fusion welding or friction stir welding, thus, novel complementary methods should be integrated with friction stir welding for reduction of residual stress. In this work, a hybrid method was introduced called bending mode ultrasonic-assisted friction stir welding (BM-UAFSW) and its effect under various vibration amplitudes was investigated on the longitudinal residual stress in a cross-section area of 3 mm and thickness of 5 mm AA6061-T6 plates using contour method. The findings indicated that BM-UAFSW can decrease the maximum longitudinal residual stress by up to 24% in relation with the conventional FSW. In addition, the reaction forces along tool axis and macrostructure observation were provided to illustrate the effect of high-frequency bending mode ultrasonic vibrations on the welding force and welding quality. All the results suggest that BM-UAFSW with amplitude of 2 and 3 μm provides the best outcome for the welding of 3 and 5 mm thick joints, respectively.

Keywords FSW · Bending mode · Ultrasonic vibration · Residual stress · Contour method

1 Introduction

Friction stir welding (FSW) as a solid-state process was first developed by The Welding Institute (TWI) in 1991 [1]. It has been the most significant development in joining of metals over the past decade and has metallurgical, environmental, and energy benefits compared to fusion welding [2]. FSW can be employed as a novel solution to welding high strength nonferrous metal such as aluminum alloys (i.e., 2XXX, 6XXX, and 7XXX series), which are basically non-weldable with conventional fusion welding due to low microstructure quality and plenty of porosity.

Like other manufacturing processes, FSW can be combined with other hybrid techniques, such as ultrasonic process, including ultrasonic-assisted friction stir welding (UA-FSW) to obtain better results (Fig 1). The research findings imply that use of ultrasonic energy in different metal-forming processes causes reduction of reaction forces, acceleration of the process, and improved quality of the products [3–5].

Few reports are available for application of ultrasonic vibration in friction stir welding. Among them, Amini and Amiri [6] investigated the effects of force, temperature, hardness, and tensile strength of 3.5 mm thick AA6061 plate. The empirical results demonstrated significant evidence of downward and forward force reduction due to better material softening. Further, the temperature outcomes indicated that US vibrations provide higher temperatures at shoulder because of better stirring performance. Furthermore, the tensile test illustrated that for low welding speeds, ultrasonic vibration cannot significantly improve the tensile strength, while at high welding speeds, it can improve tensile strength. In another work, Ahmadnia et al. [7] investigated the influence of vertical high-frequency vibration on the mechanical and the tribological properties of the AA6061 material, and they demonstrated that UV improves both characterizations.

Residual stresses (RS) refer to self-equilibrating stresses which even exist in the absence of external loads in elastic materials. Since FSW is known as a thermo-mechanical process, hence, similar to fusion welding, thermal, and mechanical stresses are produced inside the welded components. As an important parameter in welding, they can considerably affect mechanical behavior of components. Depending on the nature of stresses (i.e., compressive

✉ M. Honarpisheh
honarpishe@kashanu.ac.ir

[1] Faculty of Mechanical Engineering, University of Kashan, Kashan, Iran

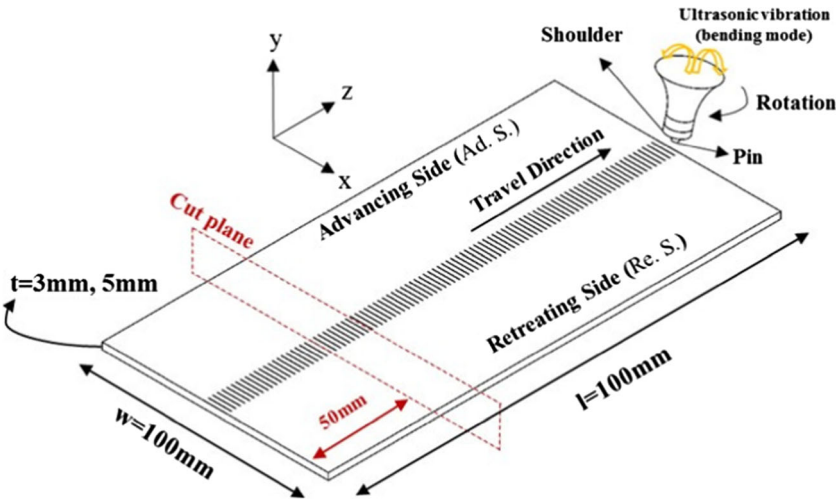

Fig. 1 Schematic of UAFSW

or tensile), it has detrimental and beneficial effects on the mechanical properties and service life of the components [8]. As an instance, Paulo et al. [9] demonstrated the influence of residual stress on the compressive strength. In another work, Citarella et al. [10] indicated that the effect of manufacturing residual stress on crack propagation in the FS welded joint by a fatigue load is predictable. In a similar way, the effect of the residual stress distribution on crack growth was analyzed by Carlone et al. [11].

The influence of residual stress owning to FSW on the structure performance has extensively been investigated with numerical and empirical techniques [12–14]. A 3D–model, based on thermo-mechanical responses, was developed in commercial software ABAQUS by Jamshidi Aval et al. [15] in order to predict residual stress on dissimilar joints, and they showed that rational speed changes maximum tensile residual stress significantly and the position of clamps affects residual stress profile. In another work, Woo and Choo [16] presented the relationship of softening behavior and residual stress profile for AA6061-T6 weld joints.

Many techniques have been employed to measure residual stress in friction stir welded components. Among them, Lombardi et al. [17] used neutron diffraction, Papahn et al. [18] employed ultrasonic waves, and Oliveira et al. [19] employed X ray diffraction as non-destructive methods to measure residual stresses produced. Also, as destructive methods, one can mention hole drilling [20, 21] and slitting methods [22–24]. In a very specific case, Liu and Yi [25] measured longitudinal residual stress for friction stir welded AA6061-T6 plates (i.e., thicknesses of 4 and 8 mm) using contour method, and they demonstrated that the maximum longitudinal stress can be brought to 61% of the yield stress of the base metal under certain conditions.

Although researchers have devoted much attention to residual stress in FSW, they have directed little attention to reduce it by novel hybrid methods such as ultrasonic vibrations. In this work, a hybrid method called bending mode ultrasonic-assisted friction stir welding is used to demonstrate the influence of high-frequency ultrasonic vibrations on longitudinal residual stress. For this approach, an experimental setup with new designed friction stir apparatus was set up on two sets of AA6061-T6 aluminum alloy plates with 3 and 5 mm thicknesses. The counter method is employed to measure longitudinal residual stress, and welding forces as well as the macrostructure of the weld zone are illustrated to indicate the influence of ultrasonic on the welding forces and quality.

2 Materials and methods

2.1 The tool

In this work, a special tool was designed and developed at Kashan University, which had three major components: tip, transducer, and piezoelectric actuators. The new tool design consisting of both ultrasonic vibration apparatus and FSW tool has the potential to develop ultrasonic waves with a bending mode during friction stir welding. Bending mode ultrasonic vibrations refer to types of high-frequency vibrations with bending formation on the tool or transducer similar to Fig. 2a. Under these vibrations, the tool oscillates horizontally or obliquely to the surface of the part. The proposed tool with bending mode vibrations has a circular locus which can cause better material flow during FSW. The difference of longitudinal vibration and bending vibration can be seen in Fig. 2a, b. The direction of vibrations in the longitudinal mode is along the axis of the tool, while it makes angle to the tool axis in the bending mode.

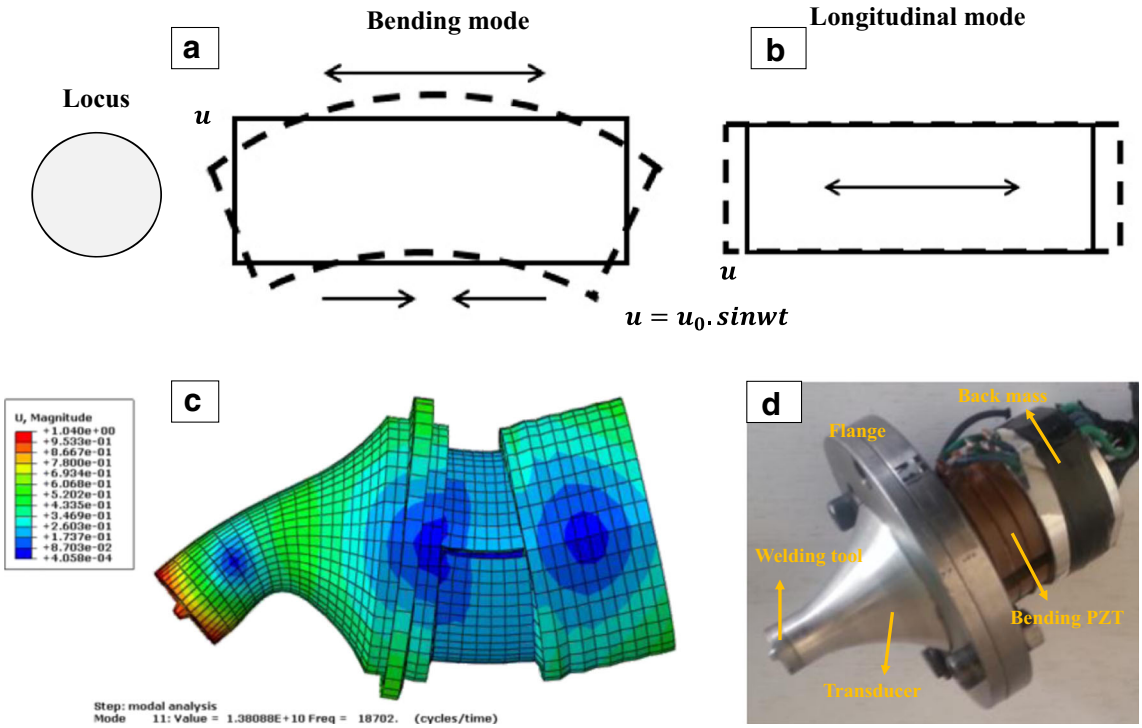

Fig. 2 Ultrasonic vibrations. **a** Bending mode. **b** Longitudinal mode. **c** Modal analysis of BM-UAFSW apparatus. **d** fabricated apparatus

The required modal analysis depicted in Fig. 2c for apparatus (tool) design was performed by commercial software ABAQUSE 6.14. As can be seen, the apparatus has the ability to produce bending vibration at a frequency of 18.70 kHz, and Fig. 2d illustrates the fabricated prototype obtained from modal analysis. The transducer and back mass have been produced from AA7075 material and other components except piezoelectric ceramics have been made from H13 steel material. There are two sets of piezoelectric ceramics, each containing four bending PZTs (half ceramics). Each set provides the required displacement in a different phase in collaboration with one another to produce bending mode vibrations similar to Fig. 2. A generator provides the periodic voltage on both sets of the piezoelectric ceramics in 180 degrees phase shift. In practice, the apparatus provides 18.5 KHz with a maximum amplitude (u_0) of 3 μm at the outer edge of the tool tip. In this work, welding is done under various amplitudes provided in Table 1. It can be seen that under condition "i" the vibration amplitude is equal to 0, meaning that FS welding was performed without using ultrasonic vibration, and welded plates are non-ultrasonic welded sample under this condition. Moreover, the welding tool (apparatus head) has pin profile due to its better stirring action. The pin has conical shape with a major diameter of 3 mm and minor diameter of 2 mm. Also, flat shoulder is considered for the apparatus head with a diameter of 18 mm.

Table 1 The welding conditions

Condition/ state	Vibration amplitude/u_0 (μm)
i	0/(without vibration)
ii	2.0
iii	2.5
iv	3.0

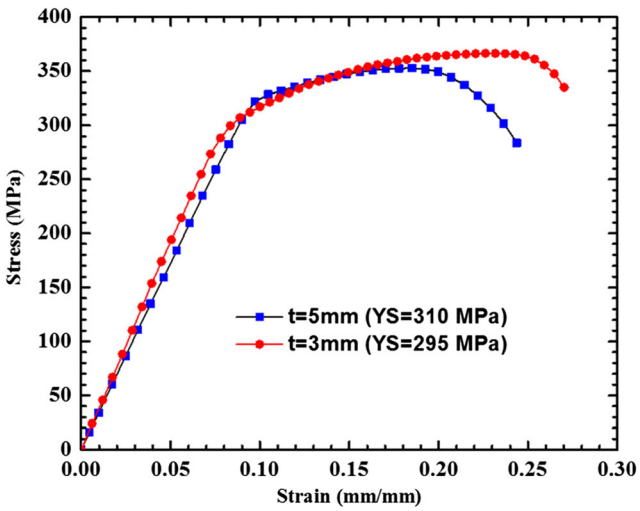

Fig. 3 Tensile test for 3 mm and 5 mm thick AA6061-T6 plates used in this study

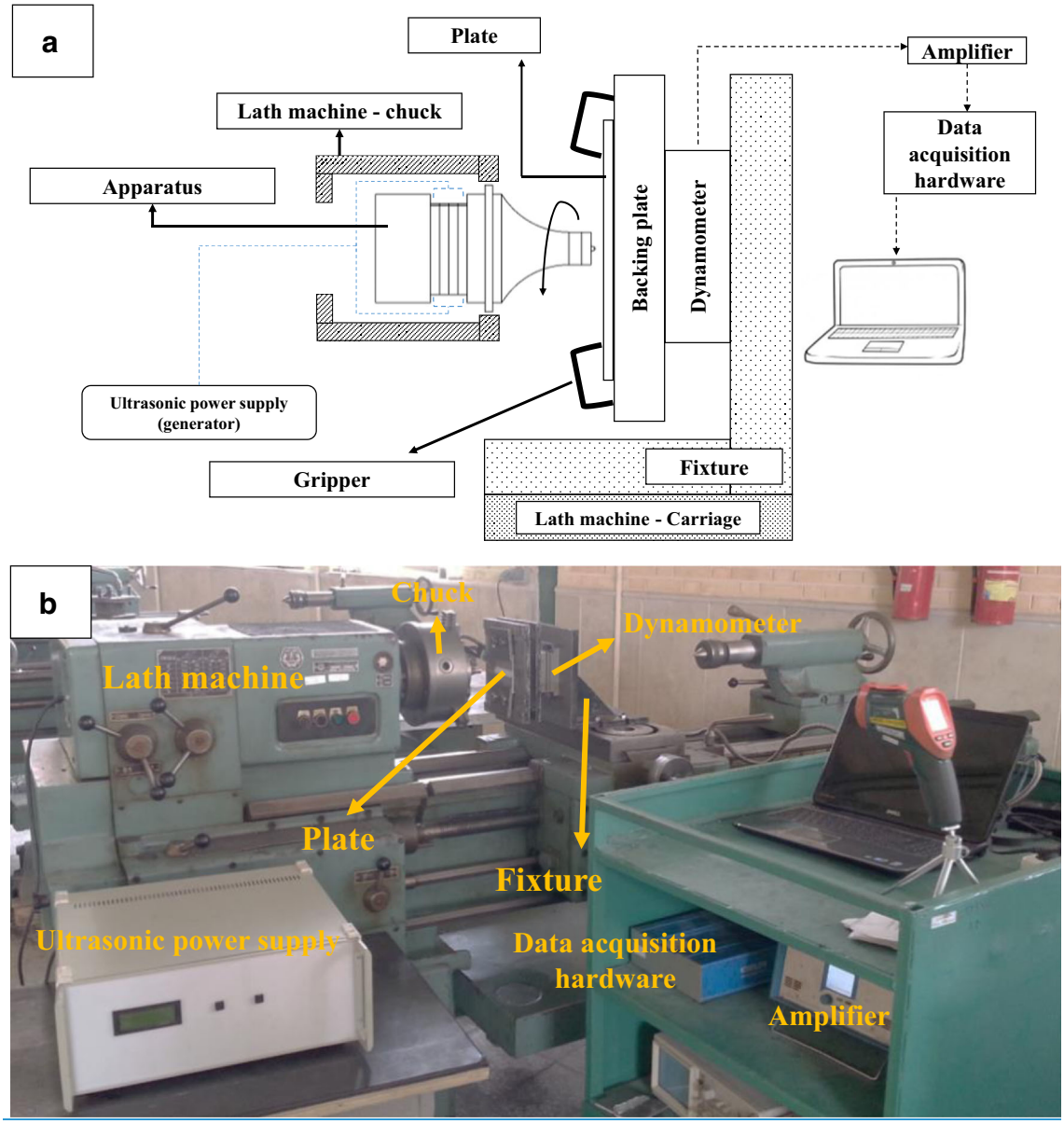

Fig. 4 The experimental setup of BM-UAFSW. **a** The schematic diagram. **b** The photo

2.2 Welding procedure

In this work, the plates of AA6061-T6 of 3 and 5 mm thickness were tailored into the required sizes (100 × 200 mm) by guillotine cutting machine (see Fig. 1). This material has been chosen due to excellent corrosion resistance and yield strength. Figure 3 illustrates the stress-strain graph for 3 mm thick and 5 mm thick AA6061-T6 plates. The UAFSW, dynamometer and fixture were mounted on Lathe machine (TN 50A), which has a maximum spindle speed of 2000 RPM and power of 5.5 kW. Further, a spindle speed of 700 RPM and traveling speed of 50 mm/min were chosen for performing FSW.

The welding axial forces have been provided by axial strike of tool into plates and measured by a KISTLER multi-component milling force dynamometer. The thrust force along tool axis was measured by a KISTLER 9257B dynamometer. The position of the dynamometer can be observed in Fig. 4. The dynamometer was directly connected to the amplifier (type 5070 A) and then, through a data acquisition hardware, it was connected to a computer (Fig. 4a). Figure 4a demonstrates a schema of the experimental setup including apparatus (i.e., FSW tool, ultrasonic transduce, etc.) generator and lath machine.

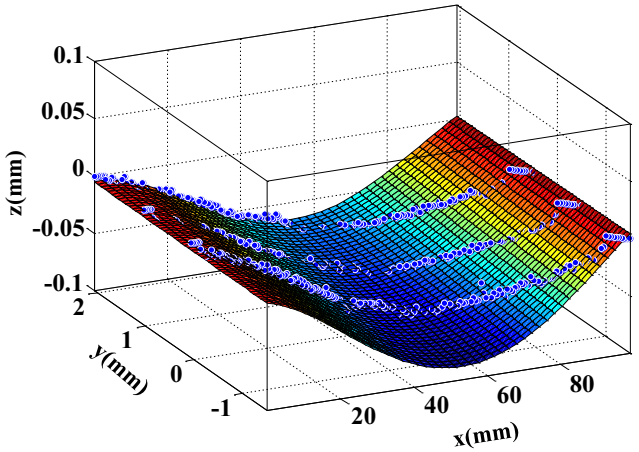

Fig. 5 Data smoothing and regression for 3 mm thick plate welded under condition ii

3 Contour method measurement

The contour method is a novel technique to measure the residual stress over a cross section. This technique determines residual stress by measuring deformed surface due to released stresses as a result of sectioning. The majority of the counter method involves the ability of 2D mapping of the residual stress across the cross-section area [26]. Generally, contour method comes with four steps: (1) specimen cutting, (2) displacement measurement, (3) data processing, and (4) FEA. In this study, these steps have been followed. In the first step, samples should be cut by a wire electric discharge machine (EDM). This process produces very straight and clean cuts and does not affect previous cut surface and does not produce any plastic deformation either. The cutting process should be performed under proper conditions to obtain the best surface roughness and less induced stress. In this study, the plates were cut with a CHARMILLES ROBOFIL 290 wire EDM machine. There are various cutting parameters for different materials and thickness. Liu and Yi [25] used 0.5 mm/min cutting speed with 0.2 mm brass wire diameter for cutting Al6061-T6 plates with 4 and 8 mm thickness. In this study, the cutting process was performed with 0.1 mm diameter brass wire and 0.5 mm/min cutting speed for both thicknesses in order to reduce possibility of induced stresses by the wire, improving the surface roughness as well. The cut plan position is demonstrated in Fig. 1, and the whole cutting process was carried out submerged in deionized water to control thermal effects (i.e., thermal stresses, distortions). The deformation of cut surface in this study was measured by a coordinate measuring machine (Sky 1 model) with an accuracy of 0.001, 0.005, and 0.0001 mm in x, y, and z directions.

The distributions of the measurement points are very important to find proper surface accuracy. For instance, Ref [25] employed a point spacing of 0.5 mm along the length and 1 mm along thickness. In another work, the residual stress was measured by contour method with a grid size of 0.5 × 0.5 mm on the cut surface [27]. Further,

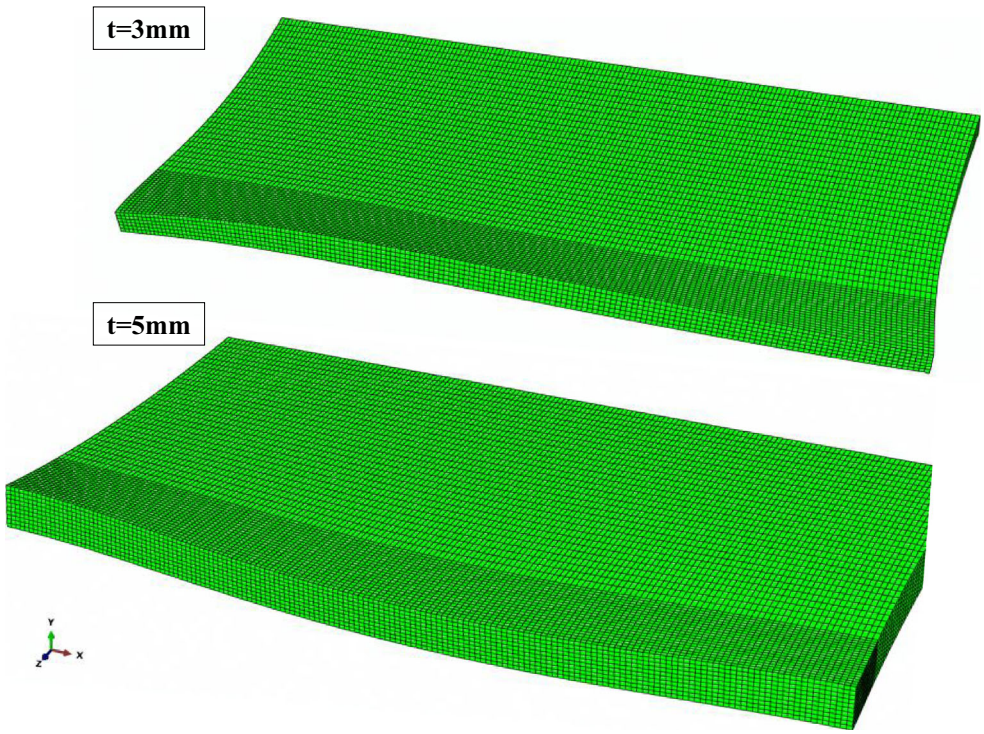

Fig. 6 3D FEA model of deformed 3 and 5 mm thick plates welded under condition ii with a deformation scale factor of 50

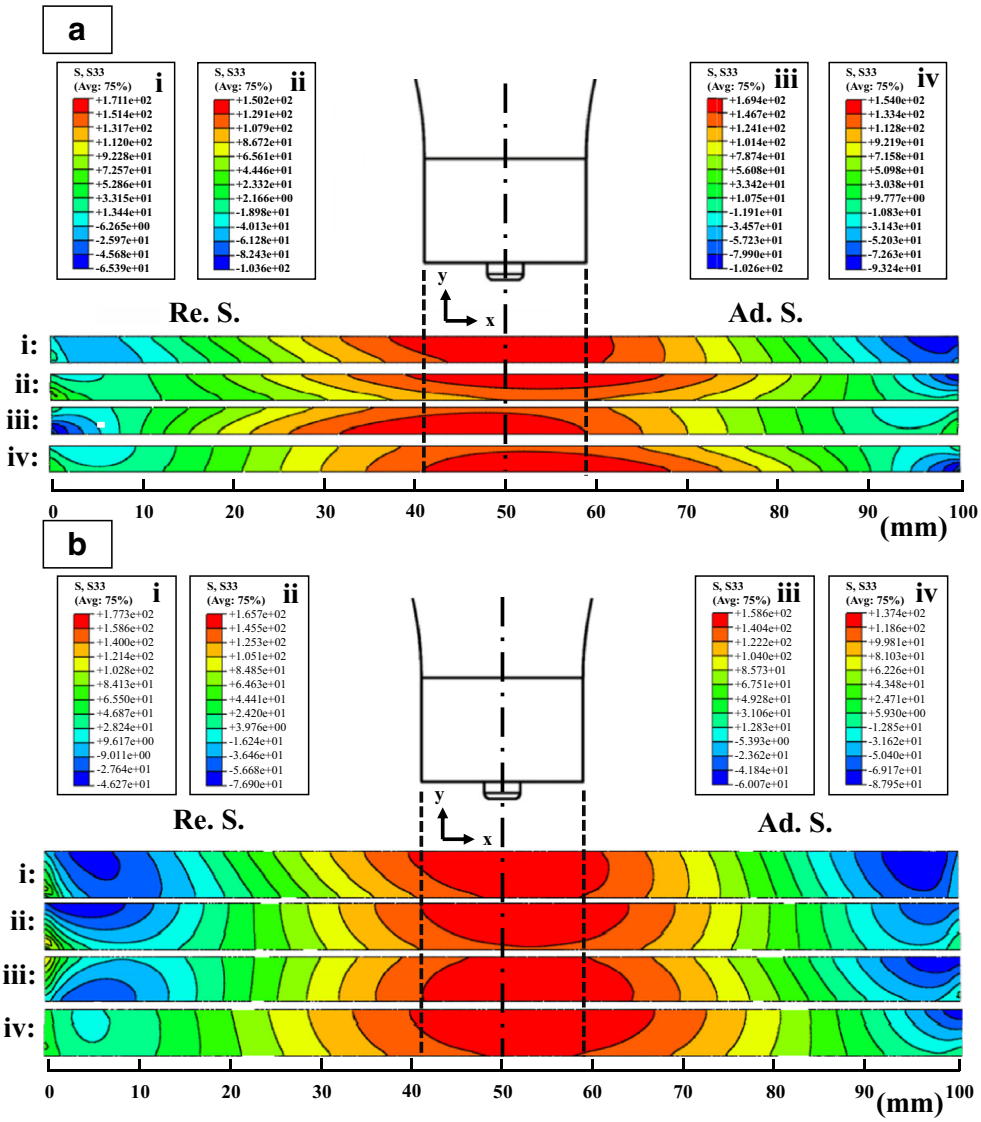

Fig. 7 Cross-sectional residual stress mapping under various welding conditions (see Table 1) for **a** 3 mm thick specimens and **b** 5 mm thick specimens

in a study [28] the point spacing of 0.5 × 0.5 mm was used to find the surface profile of welded AA22 alloy plate. Here, the point spacing was determined with 0.5 mm along the length (x direction) and 1 mm along the thickness (y direction) of cut surface for both sets of plates (3 and 5mm). This results in 200 points in the x direction and 3 points in y direction and total points of 600 for the plates with a thickness of 3 mm. Similarly, for 5 mm thick plates, a grid of 6 × 200 points results in 1000 points. Moreover, the measurement should be performed for both opposing surfaces of each cut samples. On the other hand, if there is one joint, then there are two measurement trials.

As an instance, the measured raw data (blue dotted points) for 3 mm thick joint, under condition ii, are shown in Fig. 5. It is observed that data cleaning and smoothing were employed to make the points clear and effective. There are noises in the measured points even under the best cutting and measuring conditions, and they can be considered as errors which can be omitted from the data sets using regression. Figure 5 demonstrates that the cleaned data are smoothed by polynomial regression to find the profile of cut surface as a function to ease simulation. The polynomial regressions of the fourth order for x variable and first order for y variable were considered for all cases and the 3D models of the 3 and 5 mm thick half-plates were prepared in ABAQUSE CAE 6.14 software as shown in Fig. 6 to evaluate the residual stress. The spatial function of the displacements obtained from regression was applied separately to the cross section of the provided models. The model of 5 mm thick plate contained total number 82,500 linear hexahedral elements of type C3D8R and there were 49,500 linear hexahedral elements of type C3D8R for the 3 mm thick plate model.

Figure 6 also illustrates the deformed model for 3 and 5 mm thick plates. As can be seen, the meshes in a region near to the cut surface have size of 0.5 mm and the others have a size of 1 mm.

4 Results and discussion

Longitudinal residual stress (σ_z) measurement is common in welded components. In this study, since displacement measurements have been along z direction (see Fig. 1), so the residual stresses along this direction have been presented. As the key principal advantages of the contour method include the cross-sectional mapping of the stress, then Fig. 7 demonstrates mapping of longitudinal residual stress in megapascal under different welding conditions using contour method (see Table 1). The stress mapping from Fig. 7a provides the stress distribution for 3 mm thick plates. It indicates that the longitudinal stress is tensile throughout the thickness within weld region for all cases. It can be seen that the maximum stress region under shoulder area is continuous throughout the thickness for normal welding, though welding under vibrations makes it discontinuous. It is also observed that welding under condition iii and iv pushes the maximum tensile stress to the bottom of the weld region. On the other hand, the bending mode ultrasonic vibrations with higher amplitudes can reduce tensile stress at the top of the 3-mm thick plates. Also, FS welding under condition ii produces the least residual stress compared to other conditions. Furthermore, the RSs at the top and bottom of the joint within the axis of the tool are 171 and 150 MPa for FS welding under condition i, while they are 150 MPa and 87 MPa for FS welding under condition ii, respectively. Besides, BM-UAFSW with an amplitude of 2 μm can produce 42% RS reduction between the top and bottom of the 3 mm thick joints, yet the reduction is 34% for welding without ultrasonic vibrations. Moreover, there are also compressive stress regions away from the weld region, and FS welding with ultrasonic vibrations produces higher compressive residual stress compared to normal welding at the sides of the joints which might be helpful for crack propagation in fatigue fracture [29].

Unlike 3 mm thick joints, in 5 mm ones, the RS underneath the shoulder within the thickness is continuous and FS welding under condition iv produces the least longitudinal

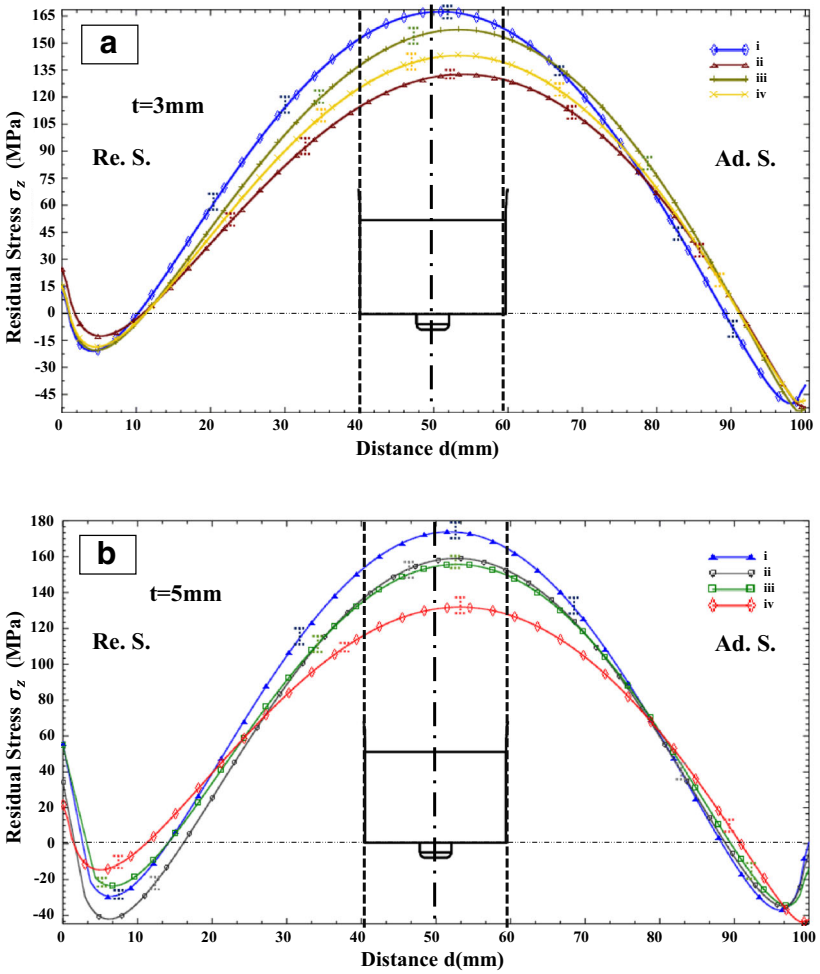

Fig. 8 Longitudinal residual stress distribution along the width and a line at the middle of the thickness on cut plane including error bar **a** 3 mm thick specimens and **b** 5 mm thick specimens

Table 2 Maximum tensile residual stress for different welding conditions and joints

FS welding conditions	$\sigma_{z,\ max}$ for 3-mm thick joints (MPa)	$\sigma_{z,\ max}$ for 5-mm thick joints (MPa)
i	173	166
ii	160	133
iii	157	158
iv	132	143

residual stress compared to other conditions. Also, the RSs at the top and bottom of the joint within the axis of the tool are 177 and 158 MPa for FS welding under condition i, while they are 137 and 118 MPa for FS welding under condition ii, respectively. On the other hand, BM-UAFSW with an amplitude of 3 μm can produce 13% RS reduction between the top and bottom of the 5 mm thick joints. However, the reduction is 10% for welding without ultrasonic vibrations.

In many studies, maximum residual stress is based on percentage of yield stress, so this approach can be followed for comparison purposes in this present work as well. The maximum tensile residual stress is about 58% of base metal yield strength for 3 and 5 mm thick joints under normal FS welding (without ultrasonic vibrations) which can be brought to 50 and 45% for 3 and 5 mm thick joints, respectively. Further, Deplus et al. [30] reported RS in 40 and 60% of the yield strength in AA6082-T6 joints. Also, Liu and Yi [25] found a maximum ratio of 50% for 8 and 4 mm thick AA6061 welds. It can be suggested that the results are similar to this study results.

Apart from cross-section stress mapping, plots should be provided in order to demonstrate the difference of the RS precisely under various conditions. Figure 8 illustrates stress distribution along x direction in the middle of the thickness including error bar, with each sample tested in three times. The error illustrates maximum 6% error for each residual stress graph in Fig. 8. The empirical results, shown in Fig. 8a, indicate that the maximum longitudinal residual stresses (σ_z) under conditions i, ii, iii, and iv are equal to 166, 133, 158, and 143 MPa, respectively (see Table 2) for 3 mm thick joints, and all have smooth M-shape like those reported in studies [25, 31]. It can be observed that the stress can decrease from 166 MPa (normal welding without vibration) to 133 MPa (FS welding under vibratory conditions with an amplitude of 2 μm). It means that the bending mode ultrasonic vibration can reduce the longitudinal residual stress by about 20% for 3 mm thick AA6061-T6 joints. Additionally, the vibration amplitude at lower levels can produce less residual stress for the 3 mm thick joints, and the peak of tensile residual stress is at advancing side, and BM-UAFSW cannot change it. Moreover, the line graphs given in Fig. 9 provides information about measured forces during BM-UAFSW. It is seen that the plunging forces are normally far greater than welding forces across all cases. Figure 9a demonstrates the axial reaction forces of the tool (along y direction) including mean value during plunging and welding for 3-mm thick plates under various vibrational states (see Table 1), indicating that applying vibration to the tools normally decreases the reaction forces due to diminished contact of the tools and the plates.

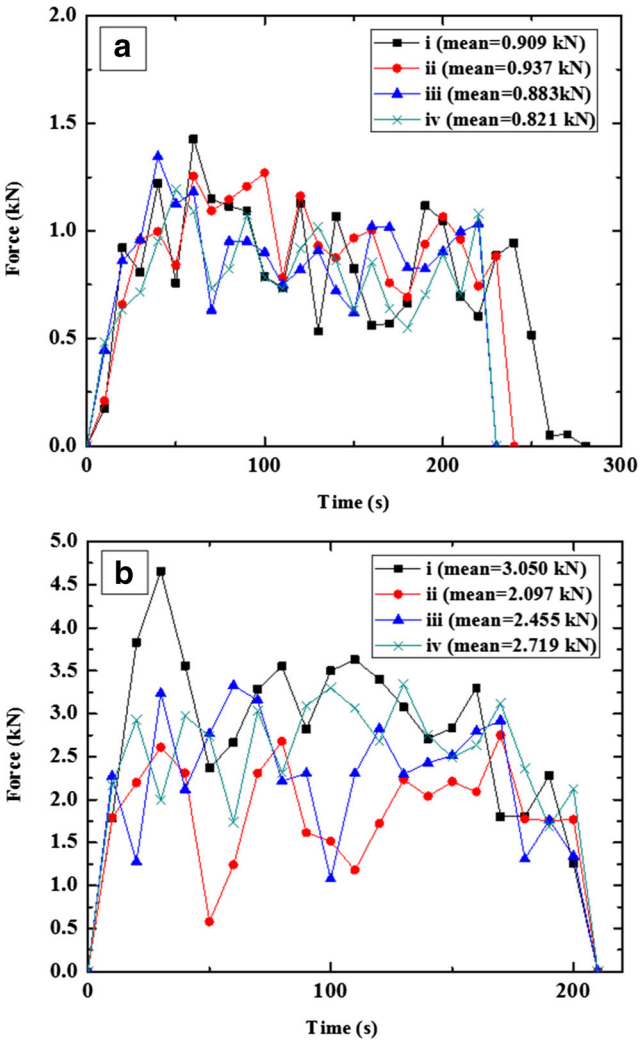

Fig. 9 Axial force for **a** 3 mm thick specimens **b** 5 mm thick specimens

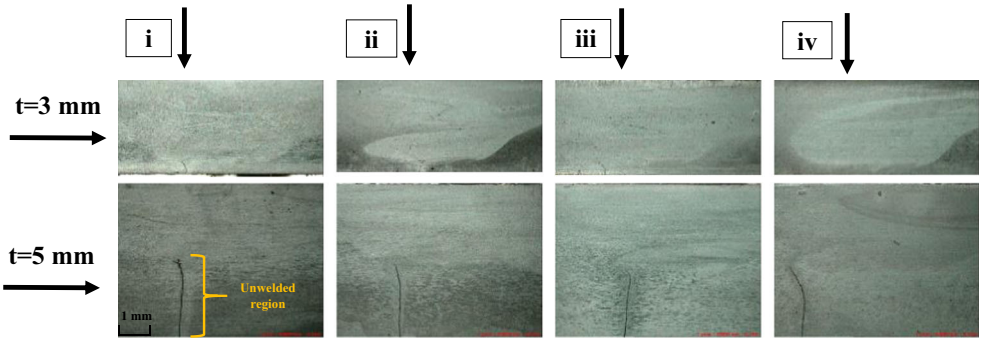

Fig. 10 Macrostructure observation of the weld zone under various conditions (see Table 1)—upper row pictures 3 mm thick plates and lower row pictures 5 mm thick plates

This would cause reduction in friction which in turn results in temperature reduction. Figure 9a indicates that the vibrations reduce axial force in 3 mm thick joints for amplitudes of more than 2.5 μm (conditions iii and iv), while the axial force increases when the amplitude is equal to 2.0 μm (condition ii). A greater axial force results better softening, which can be one of the reasons showing why maximum longitudinal residual stress is the least for case ii compared to others. It is also important to evaluate the quality of welding as macrostructure investigation. In this regard, Fig. 10 demonstrates that the ultrasonic vibrations do not significantly change the quality of welding and quality is acceptable despite few small voids.

A similar approach can be seen for 5 mm thick plates. It is, however, observed from Fig. 8a that the maximum longitudinal residual stresses (σ_z) under conditions i, ii, iii, and iv are equal to 173, 160, 157, and 132 MPa, respectively (see Table 2). This demonstrates that BM-UAFSW, under condition iv, can reduce the maximum longitudinal stress by about 24% for 5 mm thick AA6061-T6 joints. Figure 9b demonstrates that the vibrations reduce axial force in 5 mm thick joints for amplitudes of more than 2 μm (conditions ii, iii, and iv), while FS welding under state iv requires greater force compared to the two other vibratory conditions. It can be seen that although the axial force is maximum, for this case (FS welding under condition iv) the residual stress is minimum. This indicates that welding force is one of the major parameters which can affect the residual stress. Because the fiction, as a cause of heat generation and material softening, depends on the axial forces. Additionally, although FS welding under condition i has the maximum axial force, it has a greater maximum residual stress compared to others for the 5 mm thick joints. This suggests that the axial force is not the only parameter which can influence the residual stress. Hence, there should be other parameters such as the flow or the heat transfer of the materials which can have impact on the residual stress. Indeed, their impacts on the residual stress can be investigated in future works. It is observed in Fig. 9 that the welding force required for 3 mm thick plates is far less than the forced required for 5 mm plates. This is due to fact that larger amounts of material results in higher heat absorption, thereby reducing the work temperature. Therefore, reduction in work temperature reduces material softening, causing force reduction. The quality of 5 mm thick joints improve when bending mode vibration is applied such that the small voids disappear in FS welding under condition ii and iii (see Fig. 10). Moreover, it should be noted that since the same welding tool was employed for both sets of plates and the pin height was 2.5 mm, then the pin could not penetrate through the 5 mm thick joints. Thus, a seam in terms of unwelded region can be seen in all 5 mm thick joints at the weld region. The same tool was chosen to only show the effect of the vibrations without considering tool effect.

5 Conclusion

In this paper, a new hybrid method called bending mode ultrasonic-assisted friction stir welding (BM-UAFSW) was proposed to reduce residual stress. For this approach, a tool was designed and developed with the ability of producing high-frequency bending modes. This paper has mainly highlighted the influence of high-frequency bending mode ultrasonic vibration in FSW on the longitudinal residual stress, reaction force along tool axis and macrostructure of weld zone. The obtained findings are summarized as below:

- The ultrasonic vibrations in BM-UAFSW significantly reduce the tensile longitudinal residual stress for both 3 and 5 mm thick plates. It can reduce the RS approximately by up to 24%.
- The tensile longitudinal residual stress can be minimized when FSW is performed under vibratory conditions within amplitudes of 2.0 and 3.0 μm for 3 and 5 mm thick joints, respectively.
- Based on the findings, BM-UAFSW generally decreases the welding forces (reaction force along tool axis)

compared to conventional FSW. This can contribute to mitigation of heat generation and residual stress reduction.
- From a macrostructure aspect, the BM-UAFSW did not produce any significant defect for a spindle speed of 700 RPM and tool traveling speed of 50 mm/min.

References

1. Thomas WM, Nicholas ED, Needham JC, Murch MG, Temple-Smith P, Dawes CJ (1995) "Friction welding." Google Patents
2. Mishra RS, Ma ZY (2005) Friction stir welding and processing. Mater Sci Eng: R: Reports 50(1):1–78. https://doi.org/10.1016/j.mser.2005.07.001
3. Teimouri R, Baseri H (2013) Experimental study of rotary magnetic field-assisted dry EDM with ultrasonic vibration of workpiece. Int J Adv Manuf Technol 67(5–8):1371–1384. https://doi.org/10.1007/s00170-012-4573-6
4. Skoczypiec S (2011) Research on ultrasonically assisted electrochemical machining process. Int J Adv Manuf Technol 52(5–8):565–574. https://doi.org/10.1007/s00170-010-2774-4
5. Babitsky V, Kalashnikov A, Meadows A, Wijesundara AAH (2003) Ultrasonically assisted turning of aviation materials. J Mater Process Technol 132(1):157–167. https://doi.org/10.1016/S0924-0136(02)00844-0
6. Amini S, Amiri MR (2014) Study of ultrasonic vibrations' effect on friction stir welding. Int J Adv Manuf Technol 73(1–4):127–135. https://doi.org/10.1007/s00170-014-5806-7
7. Ahmadnia M, Seidanloo A, Teimouri R, Rostamiyan Y, Titrashi KG (2015) Determining influence of ultrasonic-assisted friction stir welding parameters on mechanical and tribological properties of AA6061 joints. Int J Adv Manuf Technol 78(9-12):2009–2024. https://doi.org/10.1007/s00170-015-6784-0
8. Pouget G, Reynolds AP (2008) Residual stress and microstructure effects on fatigue crack growth in AA2050 friction stir welds. Int J Fatigue 30(3):463–472. https://doi.org/10.1016/j.ijfatigue.2007.04.016
9. Paulo RMF, Carlone P, Valente RAF, Teixeira-Dias F, Palazzo GS (Jan. 2014) Influence of friction stir welding residual stresses on the compressive strength of aluminium alloy plates. Thin-Walled Struct 74:184–190. https://doi.org/10.1016/j.tws.2013.09.012
10. Citarella R, Carlone P, Lepore M, Sepe R (2016) Hybrid technique to assess the fatigue performance of multiple cracked FSW joints. Eng Fract Mech 162:38–50. https://doi.org/10.1016/j.engfracmech.2016.05.005
11. Carlone P, Citarella R, Sonne MR, Hattel JH (2016) Multiple crack growth prediction in AA2024-T3 friction stir welded joints, including manufacturing effects. Int J Fatigue 90:69–77. https://doi.org/10.1016/j.ijfatigue.2016.04.004
12. Buffa G, Ducato A, Fratini L (2011) Numerical procedure for residual stresses prediction in friction stir welding. Finite Elem Anal Des 47(4):470–476. https://doi.org/10.1016/j.finel.2010.12.018
13. Woo W, Feng Z, Wang X, David SA (2011) Neutron diffraction measurements of residual stresses in friction stir welding: a review. Sci Technol Weld Join 16(1):23–32. https://doi.org/10.1179/136217110X12731414739916
14. Fratini L, Pasta S (2011) Residual stresses in friction stir welded parts of complex geometry. Int J Adv Manuf Technol 59(5–8):547–557
15. Jamshidi Aval H, Serajzadeh S, Kokabi AH (2012) Experimental and theoretical evaluations of thermal histories and residual stresses in dissimilar friction stir welding of AA5086-AA6061. Int J Adv Manuf Technol 61(1–4):149–160. https://doi.org/10.1007/s00170-011-3713-8
16. Woo W, Choo H (2011) Softening behaviour of friction stir welded Al 6061-T6 and Mg AZ31B alloys. Science and Technology of Welding and Joining 16:267–272. https://doi.org/10.1179/1362171811Y.0000000016
17. Lombardi A, Sediako D, Machin A, Ravindran C, MacKay R (2017) Effect of solution heat treatment on residual stress in Al alloy engine blocks using neutron diffraction. Mater Sci Eng A 697:238–247. https://doi.org/10.1016/j.msea.2017.05.026
18. Papahn H, Bahemmat P, Haghpanahi M (2016) Effect of cooling media on residual stresses induced by a solid-state welding: underwater FSW. Int J Adv Manuf Technol 83(5–8):1003–1012. https://doi.org/10.1007/s00170-015-7653-6
19. Oliveira JP, Fernandes FMB, Miranda RM, Schell N, Ocaña JL (2016) Residual stress analysis in laser welded NiTi sheets using synchrotron X-ray diffraction. Mater Des 100:180–187. https://doi.org/10.1016/j.matdes.2016.03.137
20. Sedighi M, Honarpisheh M (Nov. 2012) Investigation of cold rolling influence on near surface residual stress distribution in explosive welded multilayer. Strength Mater 44(6):693–698. https://doi.org/10.1007/s11223-012-9424-z
21. He J, Ling Z, Li H (2016) Effect of tool rotational speed on residual stress, microstructure, and tensile properties of friction stir welded 6061-T6 aluminum alloy thick plate. Int J Adv Manuf Technol 84(9–12):1953–1961. https://doi.org/10.1007/s00170-015-7859-7
22. Honarpisheh M, Haghighat E, Kotobi M (2016) Investigation of residual stress and mechanical properties of equal channel angular rolled St12 strips. Proc Inst Mech Eng Part L: J Mater: Design Applic. https://doi.org/10.1177/1464420716652436
23. Kotobi M, Honarpisheh M (2017) Uncertainty analysis of residual stresses measured by slitting method in equal-channel angular rolled Al-1060 strips. J Strain Anal Eng Design 52(2):83–92. https://doi.org/10.1177/0309324716682124
24. Kotobi M, Honarpisheh M (2017) Experimental and numerical investigation of through-thickness residual stress of laser-bent Ti samples. J Strain Anal Eng Design 52(6):347–355. https://doi.org/10.1177/0309324717719212
25. Liu C, Yi X (2013) Residual stress measurement on AA6061-T6 aluminum alloy friction stir butt welds using contour method. Mater Des 46:366–371. https://doi.org/10.1016/j.matdes.2012.10.030
26. Prime MB (2001) Cross-sectional mapping of residual stresses by measuring the surface contour after a cut. J Eng Mater Technol 123(2):162
27. Turski M, Edwards L (2009) Residual stress measurement of a 316l stainless steel bead-on-plate specimen utilising the contour method. Int J Press Vessel Pip 86(1):126–131. https://doi.org/10.1016/j.ijpvp.2008.11.020
28. DeWald AT, Rankin JE, Hill MR, Lee MJ, Chen H-L (2004) Assessment of tensile residual stress mitigation in alloy 22 welds due to laser peening. J Eng Mater Technol 126(4):465
29. PASTA S, REYNOLDS AP (2008) Residual stress effects on fatigue crack growth in a Ti-6Al-4V friction stir weld. Fatigue Fract Eng Mater Struct 31(7):569–580. https://doi.org/10.1111/j.1460-2695.2008.01258.x
30. Deplus K, Simar A, Van Haver W, de Meester B (2011) Residual stresses in aluminium alloy friction stir welds. Int J Adv Manuf Technol 56(5–8):493–504. https://doi.org/10.1007/s00170-011-3210-0
31. Wang, X.L., Feng, Z., David, S. A., Spooner, S., & Hubbard, C. R. (2000). Neutron diffraction study of residual stresses in friction stir welds. In Proc. 6th Int. Conf. on 'Residual stresses', Oxford, UK